

Non-Abelian Gauge Fields and Topological Insulators in Shaken Optical Lattices

Philipp Hauke,^{1,*} Olivier Tieleman,¹ Alessio Celi,¹ Christoph Ölschläger,² Juliette Simonet,² Julian Struck,² Malte Weinberg,² Patrick Windpassinger,² Klaus Sengstock,² Maciej Lewenstein,^{1,3} and André Eckardt⁴

¹ICFO—Institut de Ciències Fotòniques, Parc Mediterrani de la Tecnologia, E-08860 Castelldefels, Spain

²Institut für Laserphysik, Universität Hamburg, Luruper Chaussee 149, D-22761 Hamburg, Germany

³ICREA—Institut Catalana de Recerca i Estudis Avançats, Lluís Companys 23, E-08010 Barcelona, Spain

⁴Max-Planck-Institut für Physik komplexer Systeme, Nöthnitzer Straße 38, D-01187 Dresden, Germany

(Received 14 May 2012; revised manuscript received 26 June 2012; published 5 October 2012)

Time-periodic driving like lattice shaking offers a low-demanding method to generate artificial gauge fields in optical lattices. We identify the relevant symmetries that have to be broken by the driving function for that purpose and demonstrate the power of this method by making concrete proposals for its application to two-dimensional lattice systems: We show how to tune frustration and how to create and control band touching points like Dirac cones in the shaken kagome lattice. We propose the realization of a topological and a quantum spin Hall insulator in a shaken spin-dependent hexagonal lattice. We describe how strong artificial magnetic fields can be achieved for example in a square lattice by employing superlattice modulation. Finally, exemplified on a shaken spin-dependent square lattice, we develop a method to create strong non-Abelian gauge fields.

DOI: 10.1103/PhysRevLett.109.145301

PACS numbers: 67.85.Lm, 03.75.Lm, 73.43.-f

Topological order and topological insulators [1] are currently at the center of interest of quantum physics, especially because of their possible applications in quantum information and spintronics [2]. For this reason, there is an ongoing search for feasible realizations of such systems inside and outside of solid-state physics. Here, ultracold ground-state atoms provide a promising playground [3] (although Rydberg-excited atoms [4], trapped ions [5], and photons in nanostructured materials [6] offer interesting alternatives). Typically, topological effects require ultrastrong gauge fields or spin-orbit-like couplings. There are several ways to achieve these with ultracold atoms, from trap rotation [7] and microrotation [8], to Berry phase imprinting [9]. In optical lattices, combining laser-induced tunneling with superlattice techniques allows for strong Abelian [10] and non-Abelian [11] gauge fields and for the realization of topological insulators [12]. So far, the first lattice experiments led to the creation of staggered flux lattices [13]. Many other groups follow this direction of research [14].

Recently, there has been a burst of interest in another, experimentally less demanding, approach, namely periodic lattice shaking. Sinusoidal shaking leads to a change of strength or even sign of the tunneling and allows us to control the Mott-insulator–superfluid transition [15,16] (for a recent work in hexagonal geometry, see Ref. [17]). While in the square lattice this introduces neither frustration nor synthetic gauge fields, in the triangular lattice a sign change of the tunneling is equivalent to a π flux Abelian field [18]. Such a system mimics frustrated antiferromagnetism, classical for weakly interacting bosons [19], and quantum in the hard-core boson limit [20], where it is expected to exhibit exotic spin-liquid phases [21]. Recently, it was demonstrated that by breaking temporal symmetries of

the shaking trajectory, one can create phases of the tunneling in an optical lattice [22,23] (see also Ref. [24]), and that in this way tunable Abelian fluxes through triangular plaquettes may be generated [22]. In this Letter, we discuss nontrivial generalizations of this approach that involve also ac-induced tunneling and spinful particles. This allows us to simulate Abelian and even non-Abelian SU(2) gauge fields in different lattice geometries, as well as topological insulators. To this, we employ nonstandard optical lattices, like kagome and spin-dependent square and hexagonal lattices, and consider scenarios based on superlattice modulation.

Basic scheme, and temporal symmetries.—We consider a system of ultracold atoms in a driven optical lattice described by the Hubbard Hamiltonian $\hat{H}(t) = -\sum_{\langle ij \rangle} J_{ij} \hat{a}_i^\dagger \hat{a}_j + \sum_i v_i(t) \hat{n}_i + \hat{H}_{os}$ with (bare) tunneling matrix elements J_{ij} and annihilation and number operators \hat{a}_i and \hat{n}_i for particles (bosons or fermions) at site i ; \hat{H}_{os} collects on-site terms describing interactions or a weak static potential. The potential $v_i(t) = v_i^\omega(t) + v_i \hbar \omega$ consists of two parts: a rapid periodic drive $v_i^\omega(t) = v_i^\omega(t + T)$ of frequency $\omega = 2\pi/T$ and zero time average $\langle v_i^\omega(t) \rangle_T = 0$ with $\langle \cdot \rangle_T \equiv \frac{1}{T} \int_0^T dt$; and (unlike in Ref. [22]) strong static energy offsets $v_i \hbar \omega$ with integers v_i . For $\hbar \omega \gg J_{ij}$ a large energy difference $v_{ij} \hbar \omega \neq 0$ (here and below we use the double-index shorthand $x_i - x_j \equiv x_{ij}$) practically prohibits tunneling between i and j , unless the resonant periodic driving leads to ac-induced tunneling (ACT) [25], as it has been observed in recent experiments [26].

A gauge transformation $\hat{U} = \exp[i \sum_i \chi_i(t) \hat{n}_i]$, where $\chi_i(t) = \chi_i^\omega(t) - v_i \omega t + \gamma_i$ with $\hbar \chi_i^\omega(t) = -\int_0^t d\tau v_i^\omega(\tau) + \langle \int_0^t d\tau v_i^\omega(\tau) \rangle_T$ and constants γ_i , leads to the new Hamiltonian $\hat{H}'(t) = \hat{U}^\dagger \hat{H} \hat{U} - i\hbar \hat{U}^\dagger (d_t \hat{U})$, which can be

approximated by its time average $\hat{H}_{\text{eff}} \equiv -\sum_{\langle ij \rangle} J_{ij}^{\text{eff}} \hat{a}_i^\dagger \hat{a}_j + \hat{H}_{\text{os}}$ if $\hbar\omega$ is large compared to both the J_{ij} and the energy scales of \hat{H}_{os} . In this treatment, the initial energy offsets $\nu_i \hbar\omega$ enter via the effective tunneling matrix elements $J_{ij}^{\text{eff}} = J_{ij} \langle e^{-i\chi_{ij}(t)} \rangle_T$ only, and in \hat{H}_{eff} all sites appear to have the same energy. In the undriven system, for $\nu_{ij} \neq 0$, the large energy difference $\nu_{ij} \hbar\omega$ suppresses tunneling between sites i and j , and this fact is reflected in \hat{H}_{eff} by a vanishing effective tunneling $J_{ij}^{\text{eff}} = 0$ at vanishing driving $\nu_{ij}^\omega = 0$. In turn, finite driving $\nu_{ij}^\omega \neq 0$ can establish coherent ACT with $J_{ij}^{\text{eff}} \neq 0$, where the energy difference $\nu_{ij} \hbar\omega$ is bridged by ν_{ij} quanta $\hbar\omega$.

The leitmotif of the present work is to use this control scheme to induce Peierls-type phases

$$\theta_{ij} = \arg(\langle e^{-i[\chi_{ij}(t) - \nu_{ij}\omega t + \gamma_{ij}]} \rangle_T) \quad (1)$$

that cannot be eliminated globally by choice of gauge, i.e., by adjusting the constants γ_i . Such nontrivial phases correspond to artificial Abelian gauge fields; the gauge-invariant magnetic flux $\phi_P \in (-\pi, \pi]$ piercing a lattice plaquette P is (modulo 2π) obtained by summing the θ_{ij} around P . We find that the *global* reflection symmetry (r) $\nu_i^\omega(-t - \tau) = \nu_i^\omega(t - \tau)$ with respect to a global time τ (using the choice $\gamma_i = -\nu_i\omega\tau$) implies trivial $\theta_{ij} = 0$. Moreover, if ACT is not involved ($\nu_{ij} = 0$), $\theta_{ij} = 0$ follows already from the *local* reflection symmetry (r') $\nu_{ij}^\omega(-t - \tau_{ij}) = \nu_{ij}^\omega(t - \tau_{ij})$ with independent local times τ_{ij} (since $\gamma_{ij} = \nu_{ij}\omega\tau = 0$, independent of τ), or from the shift antisymmetry (s) $\nu_i^\omega(t - \frac{T}{2}) = -\nu_i^\omega(t)$ (choosing $\gamma_i = 0$) [27]. Therefore, ACT significantly reduces the constraints on the driving function $\nu_i^\omega(t)$ for the creation of artificial magnetic fields. This is nicely exemplified by recent proposals where already simple sinusoidal forcing [fulfilling (r') and (s)] leads to magnetic fields when combined with ACT—provided the temporal phase of the driving can be made site dependent [thus breaking (r)] [29]. In the following, we consider experimentally feasible scenarios where the whole system is driven in phase such that both (r) and (s) are broken.

We will later generalize the scheme described in the preceding paragraphs to the case of spin-1/2 particles and show how non-Abelian gauge fields can be realized.

Homogeneous forcing and triangular plaquettes.—Let us consider a homogeneous time-periodic force $\mathbf{F}(t)$, such as an inertial force created by shaking the lattice along a periodic orbit. For $\nu_i = 0$, the driving potential $\nu_i^\omega(t) = -\mathbf{r}_i \cdot \mathbf{F}(t)$ (with site position \mathbf{r}_i) results in Peierls phases θ_{ij} that only depend on the vector $\mathbf{r}_{ij} = \mathbf{r}_i - \mathbf{r}_j$ connecting the two sites i and j , $\theta_{ij} = f(\mathbf{r}_{ij})$. Using Eq. (1), one finds that $f(-\mathbf{r}_{ij}) = -f(\mathbf{r}_{ij})$ and, therefore, homogeneous forcing cannot be used to create artificial magnetic fluxes through plaquettes with pairwise parallel edges. Since, however, generically θ_{ij} depends in a nonlinear fashion on \mathbf{r}_{ij} [$f(\mathbf{r}_{ij})$ is not of the form $\mathbf{b} \cdot \mathbf{r}_{ij}$], one can use lattice

shaking to induce a strong and tunable artificial magnetic flux ϕ_∇ through, e.g., a downwards pointing triangular plaquette ∇ . In the Supplemental Material [30], we analytically compute this flux for unidirectional forcing. The inversion of the triangular plaquette $\nabla \rightarrow \Delta$ reverses the sign of the flux, $\phi_\Delta = -\phi_\nabla$, such that staggered fluxes can be achieved in the triangular or kagome lattice as shown in Figs. 1(a) and 1(b). Since these flux configurations stem from homogeneous forcing they do not break the translational symmetry of the lattice.

Tuning the staggered flux allows one to continuously control the degree of frustration in these lattices from none for zero flux to maximum for π flux [corresponding to ferromagnetic ($-J_{ij}^{\text{eff}} < 0$) and antiferromagnetic coupling ($-J_{ij}^{\text{eff}} > 0$), respectively]. The fully frustrated regime gives rise to intriguing physics. For example, the flat lowest band of the kagome lattice makes the system extremely susceptible towards interaction-driven physics [31]; moreover, the case of hard-core bosons can be mapped to the spin-1/2 XY antiferromagnet [20] with possible spin-liquid ground states in the spatially anisotropic triangular lattice [21] and still unexplored behavior in the kagome geometry. The ability to tune continuously between zero and maximum frustration described here can, thus, be a powerful tool for the adiabatic preparation of frustrated quantum phases.

The realization of tunable staggered fluxes as shown in Figs. 1(a) and 1(b) is also interesting in its own right. In the bosonic case, deviations from π flux directly map to tunable Dzyaloshinskii-Moriya couplings in the spin picture (see, e.g., Ref. [32]). Furthermore, for finite flux $\phi_\Delta = \phi$, the three bands of the kagome lattice feature a complex band-touching structure whose topology can be controlled by the driving. This is illustrated in Fig. 2(a) for a lattice with $|J_{ij}^{\text{eff}}|$ equal to J_1 (J_2) along the horizontal (other) bonds [see Fig. 1(b)].

Topological and quantum spin Hall insulator.—Such triangular plaquette fluxes can be used to engineer a topological insulator and a quantum spin Hall insulator. Consider a spin-dependent hexagonal optical lattice as sketched in Fig. 1(c), where sites of the A (B) sublattice are energetically lifted (lowered) by $\Delta E/2$ for \uparrow particles,

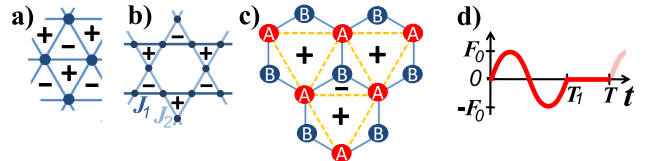


FIG. 1 (color online). (a)–(c) Lattice geometries involving triangular plaquettes pierced by an artificial magnetic flux $\phi_{\nabla,\Delta} = \pm\phi$ (indicated by + and -): (a) triangular lattice, (b) kagome lattice with tunneling J_1 (J_2) along the darker horizontal (lighter diagonal) bonds, and (c) hexagonal lattice with nearest-neighbor ACT (solid lines) between shallow A and deep B sites and next-nearest-neighbor tunneling between A sites (dashed lines). (d) Driving function $F(t)$ breaking symmetries (r) and (s).

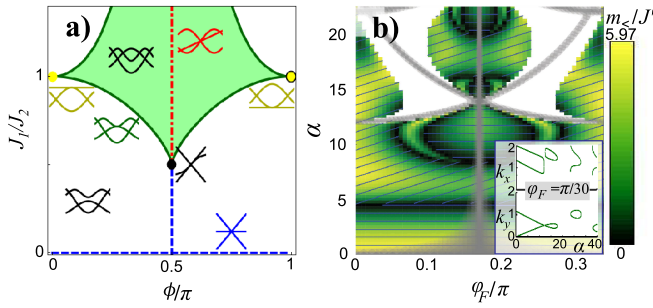


FIG. 2 (color online). (a) The topology of band touching for the kagome lattice can be controlled by anisotropy J_1/J_2 and plaquette flux ϕ . The way and how often the three bands touch is depicted by the iconographic symbols. (b) Phase diagram of the hexagonal lattice as in Fig. 1(c) with bare/undriven (next) nearest neighbor tunneling matrix elements J (J'), subjected to a symmetry-breaking force $F(t)$ of amplitude α and direction $\mathbf{e}_F = \cos(\varphi_F)\mathbf{e}_x + \sin(\varphi_F)\mathbf{e}_y$. White, no Dirac points are present; gray, a small nearest-neighbor tunneling $<0.02J$ renders the physics effectively 1D. The color bar encodes the masses at two Dirac points, labeled as $|m_{<}| \leq |m_{>}|$. In the diagonally (horizontally) hatched region both masses are positive (negative). When the masses have opposite sign (unhatched), the system is a topological insulator (or a quantum spin Hall insulator for two spin states). Inset: Position of Dirac points in k space for $\varphi_F = \pi/30$, indicating how they move and merge with α .

and vice versa for \downarrow particles [33]. Let us focus on non-interacting \uparrow particles first. For substantial detuning ΔE , we can assume that nearest-neighbor (NN) tunneling (between A and B sites) is energetically suppressed and that next-NN (NNN) tunneling is relevant only between sites of the “shallow” A sublattice. Now assume that the system is driven resonantly by a time-periodic homogeneous force of frequency $\nu_{AB}\hbar\omega = \Delta E$ (with integer ν_{AB}) that both establishes NN ACT and creates finite artificial fluxes through the triangular NNN plaquettes of the A sublattice [“+” and “-” in Fig. 1(c)]. Introducing Pauli matrices σ for the sublattice degree of freedom, the effective Hamiltonian in momentum representation becomes $\hat{H}_{\text{eff}} = \sum_{\mathbf{k}} \hat{\mathbf{a}}_{\mathbf{k}}^\dagger h(\mathbf{k}) \hat{\mathbf{a}}_{\mathbf{k}}$ where $\hat{\mathbf{a}}_{\mathbf{k}}^\dagger = (\hat{a}_{Ak}^\dagger, \hat{a}_{Bk}^\dagger)$ and $h(\mathbf{k}) = \text{Re}[g(\mathbf{k})]\sigma_x - \text{Im}[g(\mathbf{k})]\sigma_y + g'(\mathbf{k})\frac{1}{2}(1 + s_z\sigma_z)$. Here, $s_z = 1$ and $g^{(\prime)}(\mathbf{k}) \equiv -\sum_{\delta^{(l)}} J_{\delta^{(l)}}^{\text{eff}} \exp(i\mathbf{k} \cdot \delta^{(l)})$ with $\delta^{(l)}$ denoting the three (six) vectors \mathbf{k} connecting an A site to its NN (NNN). Diagonalizing $h(\mathbf{k})$ gives the dispersion relations $\varepsilon_{\pm}(\mathbf{k}) = \frac{1}{2}g'(\mathbf{k}) \pm \sqrt{|g(\mathbf{k})|^2 + |g'(\mathbf{k})/2|^2}$ for the two bands.

Without NNN tunneling ($g' = 0$), the system can possess a pair of band-touching points, i.e., $g(\mathbf{k}_{1,2}) = 0$, with light-cone-like dispersion relation, so-called Dirac cones. A finite NNN $g'(\mathbf{k})$ will split the bands at these points, and the Dirac-type dispersion relations found near $\mathbf{k}_{1,2}$ acquire finite “masses” $m_{1,2} = g'(\mathbf{k}_{1,2})$. If these have opposite sign, the lowest band possesses a finite Chern number (± 1). Then, if the lowest band is entirely filled with \uparrow fermions, the system is a topological insulator with quantized Hall conductivity and robust chiral edge modes

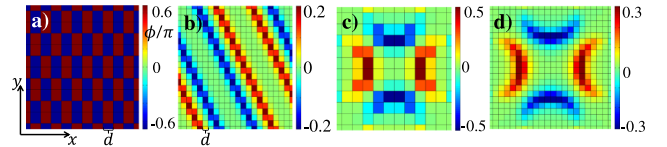


FIG. 3 (color online). Artificial magnetic fluxes ϕ through the plaquettes of a square lattice (lattice constant d , indicated by the grid) resulting from superlattice modulation. Stripes or larger patches with strong, rectified magnetic fluxes can be achieved. (a),(b) Single-component superlattices with (a) $\mathbf{q}_1 = (\pi/d)(\mathbf{e}_x + \mathbf{e}_y/2)$, $V_1 = 4\hbar\omega$; (b) $\mathbf{q}_1 = \frac{1}{10}(\pi/d)(\mathbf{e}_x + \mathbf{e}_y/2)$ and $V_1 = 20\hbar\omega$. (c) Two components with $\mathbf{q}_{1/2} = \frac{1}{10}(\pi/d)(\mathbf{e}_x \pm \mathbf{e}_y)$, $V_{1/2} = 12\hbar\omega$. (d) Like (c), but with wavelengths and amplitudes doubled. Always $\varphi_s = 0$.

[34] (see also Ref. [35]). Repeating the above reasoning for \downarrow particles, for which the role of A and B sites is interchanged, one obtains the same result, but with $s_z = -1$ and inverted Hall conductivity. Therefore, filling the lowest band with both \uparrow and \downarrow particles the system becomes a quantum spin Hall insulator with opposite chirality for the two species [36].

As an example, we consider unidirectional forcing $\mathbf{F}(t) = F(t)\mathbf{e}_F$, with $\mathbf{e}_F = \cos(\varphi_F)\mathbf{e}_x + \sin(\varphi_F)\mathbf{e}_y$ and $F(t)$ as depicted in Fig. 1(d) (with $T_1 = T/2$ and $\hbar\omega = \Delta E/2$, see Supplemental Material [30] for an analytical expression of the resulting phases). By varying the angle φ_F and the forcing strength $\alpha = dF_0T_1/(2\pi\hbar)$ (with lattice constant d), we can access various topological quantum phase transitions, where at least one of the masses vanishes and changes sign [Fig. 2(b)]. Thus, the lowest band can acquire a nontrivial Chern number. The inset shows how Dirac points can be moved and merged.

A way to measure the topological band structure of the system is given by the method of Ref. [37] based on semiclassical wave-packet dynamics. It can be applied thanks to the adiabatic principle for Floquet systems [38] (see Ref. [39] for its application to the effective Hamiltonian).

Superlattice modulation and flux rectification.—In lattices with pairwise parallel bonds, such as square lattices, homogeneous driving $\mathbf{v}_i^\omega(t) = -\mathbf{F}(t) \cdot \mathbf{r}_i$ as considered in the previous paragraphs cannot create magnetic fluxes. Therefore, we propose to drive the system via an oscillating superlattice potential $v_i(t) = f(t)V_0(\mathbf{r}_i) = f(t)\sum_s \frac{V_s}{2} \cos(\mathbf{q}_s \cdot \mathbf{r} - \varphi_s)$, where $V_0(\mathbf{r})$ may be incommensurate with the host lattice. The driving function $f(t) = f(t+T)$ breaks symmetries (r) and (s). To achieve a vanishing mean, $\langle f(t) \rangle_T = 0$, in an experiment one can use π -shifted noninterfering standing waves such that $f(t)V_s \cos(\mathbf{q}_s \cdot \mathbf{r} - \varphi_s) = V_s^l(t) \cos(\mathbf{q}_s \cdot \mathbf{r} - \varphi_s) + V_s^r(t) \cos(\mathbf{q}_s \cdot \mathbf{r} - \varphi_s + \pi)$, with $V_s^l, V_s^r > 0$. In Fig. 3, we show—on the example of a square lattice with a shaking function as in Fig. 1(d) (with $T_1/T = 0.8$)—that, using different superlattice structures, various configurations of plaquette fluxes can be engineered [40]. Roughly, the

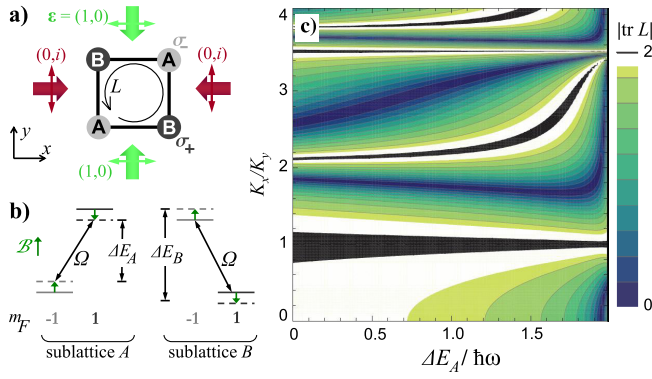


FIG. 4 (color online). Non-Abelian SU(2) gauge fields. (a) Two standing laser waves (with a phase shift of $\pi/2$ and in-plane polarization as denoted in the figure) create a bipartite square lattice with alternating σ^+ and σ^- polarized sites (A and B) [43]. $m_F = \pm 1$ particles feel an energy difference of $\pm \Delta E$ between A and B sites. (b) The resulting level scheme. A constant B field realizes an additional on-site energy splitting $\Delta E'$ (green arrow) such that $|\Delta E_{A,B}| = |\pm \Delta E + \Delta E'|$ becomes sublattice dependent. The coupling Ω of both spin states can be realized by magnetic or microwave fields. (c) Trace of the Wilson loop L in parameter space. Deviations from 2 imply non-Abelian physics [$K_y = 1.814$; outside the white (black) regions, $|\text{tr}L| < 1.9$ (< 1.99)].

larger the superlattice wavelengths the slower is the variation of the artificial flux. Therefore, superlattice modulation can generate not only strong magnetic fluxes through square plaquettes, but also large regions (stripes or patches) with rectified magnetic field where strong-field quantum Hall-type physics can be studied. Their inhomogeneity and finite extent provide a promising test ground for the investigation of robust edge modes.

Non-Abelian SU(2) gauge fields.—The periodic driving also permits the creation of arbitrary *non-Abelian* SU(2) gauge fields. Consider \uparrow and \downarrow particles (say, $m_F = \pm 1$) loaded into the spin-dependent square lattice depicted in Fig. 4(a), where the energy of \uparrow particles is lifted (lowered) by $\Delta E/2$ on A (B) sites, and vice versa for \downarrow particles. These energy shifts are summarized by $\Delta E \sigma_z s_z/2$, if we introduce two sets of Pauli matrices s and σ for spin (\uparrow or \downarrow) and sublattice (A or B), respectively. Moreover, uniform microwave and magnetic fields can be employed to couple the \uparrow and \downarrow state with a matrix element Ω and to produce an additional site-independent energy splitting $\Delta E'$, giving the site-independent term $\Delta E' s_z/2 + \Omega s_x$. The absolute value of the total \uparrow - \downarrow splitting $\Delta E_i = \Delta E \sigma_z - \Delta E'$ is sublattice-dependent [Fig. 4(b)]. Including the NN tunneling J and a spin-independent sinusoidal drive $v_i^\omega(t) = -\mathbf{r}_i \cdot \mathbf{F}_0 \cos(\omega t)$ as it can be induced by simply shaking the lattice back and forth, the Hamiltonian reads $\hat{H} = -\sum_{\langle ij \rangle} J \hat{a}_i^\dagger \hat{a}_j + \sum_i \hat{a}_i^\dagger [\frac{1}{2} \Delta E_i s_z + \Omega s_x + v_i^\omega(t)] \hat{a}_i$, with $\hat{a}_i^\dagger = (\hat{a}_{i\uparrow}^\dagger, \hat{a}_{i\downarrow}^\dagger)$. The transformation $\hat{b}_i = u_i^\dagger \hat{a}_i$, where u_i are time-independent unitary 2×2 matrices, diagonalizes the Hamiltonian on site

with eigenvalues $\hbar \lambda_i = \frac{1}{2} \sqrt{\Delta E_i^2 + 4\Omega^2}$. This yields $\hat{H} = -\sum_{\langle ij \rangle} J \hat{b}_i^\dagger u_i^\dagger u_j \hat{b}_j + \sum_i \hat{b}_i^\dagger [\hbar \lambda_i s_z + v_i^\omega(t)] \hat{b}_i$. The sublattice dependence of u_i through $\Delta E_i/(2\Omega)$ achieves generically $u_i^\dagger u_j \neq 1$. As in the derivation preceding Eq. (1), the unitary transformation $\exp\{-i \sum_i \hat{b}_i^\dagger [\lambda_i t s_z - K_i \sin(\omega t)] \hat{b}_i\}$ with $K_i = \mathbf{r}_i \cdot \mathbf{F}_0/(\hbar \omega)$ leads to a purely kinetic Hamiltonian $\hat{H}' = -\sum_{\langle ij \rangle} J \hat{b}_i^\dagger W_{ij}(t) \hat{b}_j$. Here,

$$W_{ij}(t) = e^{-i K_{ij} \sin(\omega t)} \begin{pmatrix} c_{ij} e^{i(\lambda_i - \lambda_j)t} & d_{ij} e^{-i(\lambda_i + \lambda_j)t} \\ -d_{ij}^* e^{i(\lambda_i + \lambda_j)t} & c_{ij}^* e^{-i(\lambda_i - \lambda_j)t} \end{pmatrix},$$

and c_{ij} and d_{ij} parametrize $u_i^\dagger u_j$. For $\hbar \omega \gg J_{ij}$, we can approximate \hat{H}' by its time average $\hat{H}_{\text{eff}} = \langle \hat{H}' \rangle_T = -\sum_{\langle ij \rangle} J_{ij}^{\text{eff}} \hat{b}_i^\dagger M_{ij} \hat{b}_j$, with the effective tunneling matrix elements $J_{ij}^{\text{eff}} = J \sqrt{|\det(\langle W_{ij} \rangle_T)|}$, and the matrices $M_{ij} \equiv \langle W_{ij} \rangle_T / \sqrt{|\det(\langle W_{ij} \rangle_T)|}$. For $J_{ij}^{\text{eff}} \neq 0$, we require $\lambda_{i \in B} \pm \lambda_{i \in A} = \nu_\pm \omega$ with integers ν_\pm , and for unitarity of M_{ij} , we require ν_\pm both either odd or even.

If the so called Wilson loop L , the product of the matrices M_{ij} around a plaquette, yields not just a simple phase $e^{i\phi} 1$ describing an Abelian magnetic flux ϕ , the system is subjected to a genuine non-Abelian SU(2) gauge field. This is equivalent to requiring $|\text{tr}L| < 2$, a *sine qua non* for the anomalous integer quantum Hall effect [41] and fractional quantum Hall states with non-Abelian anyonic excitations [42]. Without driving, $|\text{tr}L| = 2$, but including it, $|\text{tr}L| < 2$ can be fulfilled (see Ref. [30]).

Let us choose $\nu_+ = 3$ and $\nu_- = 1$, achieved by $\Delta E_B = \sqrt{4(\hbar \omega)^2 + \Delta E_A^2}$ and $\Omega = \sqrt{(\hbar \omega)^2 - \Delta E_A^2}/4$. This leaves $\Delta E_A/\hbar \omega$, K_x , and K_y as free parameters (where $K_{x,y}$ is the amplitude of the forcing K_{ij} in positive x, y direction). In Fig. 4(c), we plot the trace of the Wilson loop $|\text{tr}L|$ versus K_x/K_y and $E_A/\hbar \omega$ for $K_y = 1.84$ (this value is not crucial but ensures large y tunneling—see Supplemental Material [30], where also an analytical expression for the Wilson loop is derived). There are broad regions where $|\text{tr}L|$ differs strongly from 2, proving the presence of a strong artificial non-Abelian gauge field. Under typical conditions, the system shows Dirac cones, be it Abelian or non-Abelian. Similar analytic calculations reveal that $L \equiv 1$ in a hexagonal lattice. This limitation can be overcome by employing position-dependent coupling via Raman laser mixing, $\Omega \rightarrow \Omega_i = \Omega e^{i\mathbf{q} \cdot \mathbf{r}_i}$ with \mathbf{q} the laser wave-vector difference (see Ref. [30]). This way, the M_{ij} as well as L can be tuned to be a generic $(i \times i)$ SU(2) matrix both in square and hexagonal lattices. Alternatively, in a hexagonal lattice a nontrivial Wilson loop can be achieved with NNN tunneling.

Conclusion.—The creation of artificial Abelian and non-Abelian gauge fields by means of time-periodic forcing opens realistic perspectives for experimental studies. This method offers great flexibility, because it does not involve

the internal atomic structure. For fermions, where only different internal states interact with each other, this can be very advantageous for reaching the strongly correlated regime.

We acknowledge support from AAIL-Hubbard, Spanish MICINN (FIS2008-00784), Catalunya-Caixa, EU Projects AQUATE and NAMEQUAM, ERC grant QUAGATUA, Netherlands Organisation for Scientific Research (NWO), Humboldt Stiftung, German Science Foundation (Grants No. FOR 801 and No. SFB 925), and the Hamburg Theory Prize.

*philipp.hauke@icfo.es

- [1] M. Z. Hasan and C. L. Kane, *Rev. Mod. Phys.* **82**, 3045 (2010).
- [2] C. Nayak, S. H. Simon, A. Stern, M. Freedman, and S. Das Sarma, *Rev. Mod. Phys.* **80**, 1083 (2008).
- [3] M. Lewenstein, A. Sanpera, and V. Ahufinger, *Ultracold Atoms in Optical Lattices: Simulating Quantum Many-Body Systems* (Oxford University Press, Oxford, 2012).
- [4] H. Weimer, M. Müller, I. Lesanovsky, P. Zoller, and H. P. Büchler, *Nature Phys.* **6**, 382 (2010).
- [5] J. T. Barreiro, M. Müller, P. Schindler, D. Nigg, T. Monz, M. Chwalla, M. Hennrich, C. F. Roos, P. Zoller, and R. Blatt, *Nature (London)* **470**, 486 (2011).
- [6] T. Kitagawa, M. A. Broome, A. Fedrizzi, M. S. Rudner, E. Berg, I. Kassal, A. Aspuru-Guzik, E. Demler, and A. G. White, *Nature Commun.* **3**, 882 (2012); A. Aspuru-Guzik and P. Walther, *Nature Phys.* **8**, 285 (2012).
- [7] A. L. Fetter, *Rev. Mod. Phys.* **81**, 647 (2009).
- [8] A. S. Sørensen, E. Demler, and M. D. Lukin, *Phys. Rev. Lett.* **94**, 086803 (2005); L.-K. Lim, C. Morais Smith, and A. Hemmerich, *Phys. Rev. Lett.* **100**, 130402 (2008); L.-K. Lim, A. Lazarides, A. Hemmerich, and C. Morais Smith, *Phys. Rev. A* **82**, 013616 (2010); T. Kitagawa, E. Berg, M. Rudner, and E. Demler, *Phys. Rev. B* **82**, 235114 (2010).
- [9] J. Dalibard, F. Gerbier, G. Juzeliunas, and P. Öhberg, *Rev. Mod. Phys.* **83**, 1523 (2011); Y.-J. Lin, R. L. Compton, K. Jiménez-García, J. V. Porto, and I. B. Spielman, *Nature (London)* **462**, 628 (2009); Y.-J. Lin, K. Jiménez-García, and I. B. Spielman, *Nature (London)* **471**, 83 (2011).
- [10] D. Jaksch and P. Zoller, *New J. Phys.* **5**, 56 (2003).
- [11] K. Osterloh, M. Baig, L. Santos, P. Zoller, and M. Lewenstein, *Phys. Rev. Lett.* **95**, 010403 (2005).
- [12] L. Mazza, A. Bermudez, N. Goldman, M. Rizzi, M. A. Martin-Delgado, and M. Lewenstein, *New J. Phys.* **14**, 015007 (2012).
- [13] M. Aidelsburger, M. Atala, S. Nascimbène, S. Trotzky, Y.-A. Chen, and I. Bloch, *Phys. Rev. Lett.* **107**, 255301 (2011).
- [14] L. Tarruell, D. Greif, T. Uehlinger, G. Jotzu, and T. Esslinger, *Nature (London)* **483**, 302 (2012); G.-B. Jo, J. Guzman, C. K. Thomas, P. Hosur, A. Vishwanath, and D. M. Stamper-Kurn, *Phys. Rev. Lett.* **108**, 045305 (2012).
- [15] A. Eckardt, C. Weiss, and M. Holthaus, *Phys. Rev. Lett.* **95**, 260404 (2005).
- [16] H. Lignier, C. Sias, D. Ciampini, Y. Singh, A. Zenesini, O. Morsch, and E. Arimondo, *Phys. Rev. Lett.* **99**, 220403 (2007); A. Zenesini, H. Lignier, D. Ciampini, O. Morsch, and E. Arimondo, *Phys. Rev. Lett.* **102**, 100403 (2009).
- [17] S. Koghee, L.-K. Lim, M. O. Goerbig, and C. Morais Smith, *Phys. Rev. A* **85**, 023637 (2012).
- [18] V. Kalmeyer and R. B. Laughlin, *Phys. Rev. Lett.* **59**, 2095 (1987).
- [19] J. Struck, C. Ölschläger, R. Le Targat, P. Soltan-Panahi, A. Eckardt, M. Lewenstein, P. Windpassinger, and K. Sengstock, *Science* **333**, 996 (2011).
- [20] A. Eckardt, P. Hauke, P. Soltan-Panahi, C. Becker, K. Sengstock, and M. Lewenstein, *Europhys. Lett.* **89**, 10010 (2010).
- [21] R. Schmied, T. Roscilde, V. Murg, D. Porras, and J. I. Cirac, *New J. Phys.* **10**, 045017 (2008); P. Hauke, T. Roscilde, V. Murg, J. Ignacio Cirac, and R. Schmied, *New J. Phys.* **12**, 053036 (2010).
- [22] J. Struck, C. Ölschläger, M. Weinberg, P. Hauke, J. Simonet, A. Eckardt, M. Lewenstein, K. Sengstock, and P. Windpassinger, *Phys. Rev. Lett.* **108**, 225304 (2012).
- [23] K. Sacha, K. Targońska, and J. Zakrzewski, *Phys. Rev. A* **85**, 053613 (2012).
- [24] K. Jiménez-García, L. J. LeBlanc, R. A. Williams, M. C. Beeler, A. R. Perry, and I. B. Spielman, *Phys. Rev. Lett.* **108**, 225303 (2012).
- [25] A. Eckardt and M. Holthaus, *Europhys. Lett.* **80**, 50004 (2007).
- [26] C. Sias, H. Lignier, Y. P. Singh, A. Zenesini, D. Ciampini, O. Morsch, and E. Arimondo, *Phys. Rev. Lett.* **100**, 040404 (2008); A. Alberti, V. V. Ivanov, G. M. Tino, and G. Ferrari, *Nature Phys.* **5**, 547 (2009); E. Haller, R. Hart, M. J. Mark, J. G. Danzl, L. Reichsöllner, and H.-C. Nägerl, *Phys. Rev. Lett.* **104**, 200403 (2010); R. Ma, M. Eric Tai, P. M. Preiss, W. S. Bakr, J. Simon, and M. Greiner, *Phys. Rev. Lett.* **107**, 095301 (2011).
- [27] See Refs. [22,28] for connections to ratchet physics.
- [28] S. Flach, O. Yevtushenko, and Y. Zolotaryuk, *Phys. Rev. Lett.* **84**, 2358 (2000); S. Denisov, L. Morales-Molina, S. Flach, and P. Hänggi, *Phys. Rev. A* **75**, 063424 (2007).
- [29] A. R. Kolovsky, *Europhys. Lett.* **93**, 20003 (2011); A. Bermudez, T. Schaetz, and D. Porras, *New J. Phys.* **14**, 053049 (2012).
- [30] See Supplemental Material at <http://link.aps.org/supplemental/10.1103/PhysRevLett.109.145301> for an analytic calculation of J_{ij}^{eff} and θ_{ij} , and for technical details on the creation of non-Abelian SU(2) gauge fields.
- [31] S. D. Huber and E. Altman, *Phys. Rev. B* **82**, 184502 (2010).
- [32] L. Messio, O. Cepas, and C. Lhuillier, *Phys. Rev. B* **81**, 064428 (2010).
- [33] P. Soltan-Panahi, J. Struck, P. Hauke, A. Bick, W. Plenkers, G. Meineke, C. Becker, P. Windpassinger, M. Lewenstein, and K. Sengstock, *Nature Phys.* **7**, 434 (2011).
- [34] F. D. M. Haldane, *Phys. Rev. Lett.* **61**, 2015 (1988).
- [35] E. Alba, X. Fernandez-Gonzalvo, J. Mur-Petit, J. K. Pachos, and J. J. Garcia-Ripoll, *Phys. Rev. Lett.* **107**, 235301 (2011); T. Kitagawa, T. Oka, A. Brataas, L. Fu, and E. Demler, *Phys. Rev. B* **84**, 235108 (2011); N. Goldman, I. Satija, P. Nikolic, A. Bermudez, M. A. Martin-Delgado, M. Lewenstein, and I. B. Spielman, *Phys. Rev. Lett.* **105**, 255302 (2010).

- [36] C.L. Kane and E.J. Mele, *Phys. Rev. Lett.* **95**, 226801 (2005).
- [37] H.M. Price and N.R. Cooper, *Phys. Rev. A* **85**, 033620 (2012).
- [38] H.P. Breuer and M. Holthaus, *Phys. Lett. A* **140**, 507 (1989).
- [39] A. Eckardt and M. Holthaus, *Phys. Rev. Lett.* **101**, 245302 (2008).
- [40] For long superlattice wave lengths $|q_s d| \ll \pi$ [applies to Figs. 3(b)–3(d)], the flux through a plaquette at \mathbf{r} is given by $\phi(\mathbf{r}) \simeq \frac{1}{2} w_{xy}(\mathbf{r}) \{ \theta' [w_y(\mathbf{r})] - \theta' [w_x(\mathbf{r})] \}$, where a prime indicates the derivative, and where $w_{\mu\nu}(\mathbf{r}) = d^2 \partial_\mu \partial_\nu V(\mathbf{r}) / (\hbar\omega)$ and $w_\mu = d \partial_\mu V(\mathbf{r}) / (\hbar\omega)$.
- [41] N. Goldman, A. Kubasiak, A. Bermudez, P. Gaspard, M. Lewenstein, and M. A. Martin-Delgado, *Phys. Rev. Lett.* **103**, 035301 (2009).
- [42] M. Burrello and A. Trombettoni, *Phys. Rev. Lett.* **105**, 125304 (2010).
- [43] A. Hemmerich and T. W. Hänsch, *Phys. Rev. Lett.* **70**, 410 (1993).